

Publication Charges and Reprints

There has been a change in our author billing and reprint ordering system. Publication charges and reprint orders are now handled by Dartmouth Journal Services using a web-based system.

Within the next 24 hours you will receive an e-mail from aubilling.djs@sheridan.com. This e-mail will include a link to an online reprint order form and to an estimate of your publication charges. From this secure website you will be able to review the estimated charges for your article and order reprints. Please log in to this website as soon as possible to ensure that there will be no delay to your article being published.

Please note that this is a change in procedure. If you have questions regarding this change, about the e-mail you will receive, or about the website, please contact aubilling.djs@sheridan.com or call 802-560-8518.

Annotating PDFs using Adobe Reader XI

Version 1.4 January 14, 2014

1. Update to Adobe Reader XI

The screen images in this document were captured on a Windows PC running Adobe Reader XI. Editing of DJS proofs requires the use of Acrobat or Reader XI or higher. At the time of this writing, Adobe Reader XI is freely available and can be downloaded from <http://get.adobe.com/reader/>

2. What are eProofs?

eProof files are self-contained PDF documents for viewing on-screen and for printing. They contain all appropriate formatting and fonts to ensure correct rendering on-screen and when printing hardcopy. DJS sends eProofs that can be viewed, annotated, and printed using the free version of Acrobat Reader XI (or higher).

3. Comment & Markup toolbar functionality

A. Show the Comment & Markup toolbar

The Comment & Markup toolbar doesn't appear by default. Do one of the following:

- Select View > Comment > Annotations.
- Click the Comment button in the Task toolbar.

Note: If you've tried these steps and the Annotation Tools do not appear, make sure you have updated to version XI or higher.

B. Select a commenting or markup tool from the Annotations window.

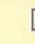

Note: After an initial comment is made, the tool changes back to the Select tool so that the comment can be moved, resized, or edited. (The Pencil, Highlight Text, and Line tools stay selected.)

C. Keep a commenting tool selected

Multiple comments can be added without reselecting the tool. Select the tool to use (but don't use it yet).

- Right Click on the tool.
- Select Keep Tool Selected.

4. Using the comment and markup tools

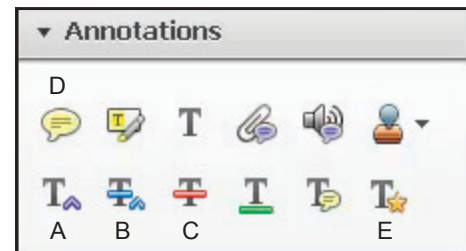
To *insert*, *delete*, or *replace* text, use the corresponding tool. Select the tool, then select the text with the cursor (or simply position it) and begin typing. A pop-up note will appear based upon the modification (e.g., inserted text, replacement text, etc.). Use the Properties bar to format text in pop-up notes. A pop-up note can be minimized by selecting the  button inside it. A color-coded  symbol will remain behind to indicate where your comment was inserted, and the comment will be visible in the Comments List.

5. The Properties bar

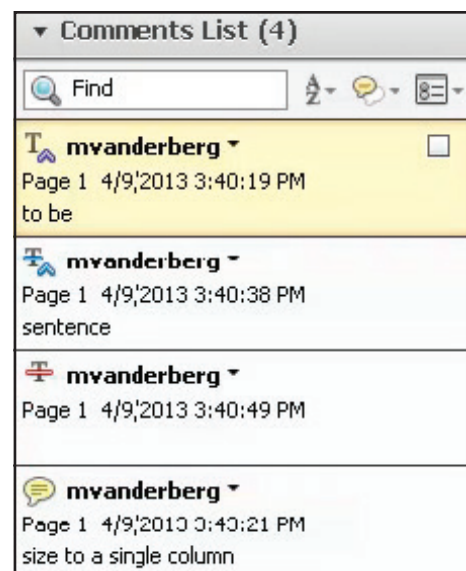
The Properties bar can be used to add formatting such as bold or italics to the text in your comments.

To view the Properties bar, do one of the following:

- Right-click the toolbar area; choose Properties Bar.
- Press [Ctrl-E]



- A. Insert Text tool
- B. Replace Text tool
- C. Delete Text tool
- D. Sticky Note tool
- E. Text Correction Markup tool



6. Inserting symbols or special characters

An 'insert symbol' feature is not available for annotations, and copying/pasting symbols or non-keyboard characters from Microsoft Word does not always work. Use angle brackets < > to indicate these special characters (e.g., <alpha>, <beta>).

7. Editing near watermarks and hyperlinked text

eProof documents often contain watermarks and/or hyperlinked text. Selecting characters near these items can be difficult using the mouse alone. To edit an eProof which contains text in these areas, do the following:

- Without selecting the watermark or hyperlink, place the cursor near the area for editing.
- Use the arrow keys to move the cursor beside the text to be edited.
- Hold down the shift key while simultaneously using arrow keys to select the block of text, if necessary.
- Insert, replace, or delete text, as needed.

8. Summary of main functions

- A. Insert text - Use Insert Text tool (position cursor and begin typing)
- B. Replace text - Use Replace Text tool (select text and begin typing)
- C. Delete text - Use Strikethrough Text tool (select text and press delete key)
Note: The Text Correction Markup tool combines the functions of all three tools.
- D. Sticky Note - Use Sticky Note tool to add comments not related to text correction.

9. Reviewing changes

To review all changes, do the following:

- Click the Comments button to reveal the comment tools
- Click the triangle next to Comments List (if not already visible)

Note: Selecting a correction in the list will highlight the corresponding item in the document, and vice versa.

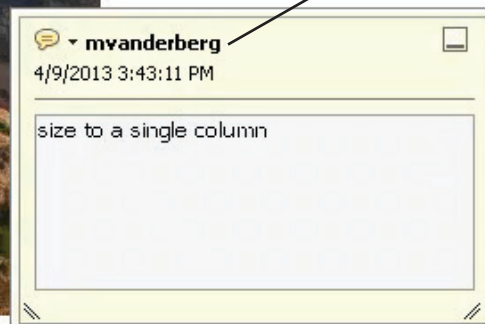
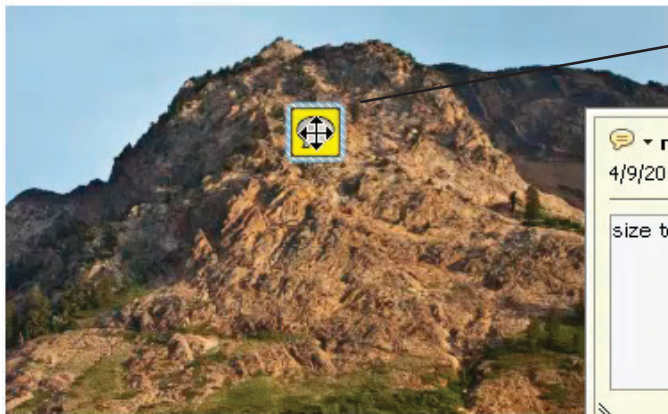
10. Still have questions?

Try viewing our brief training video at <https://authorcenter.dartmouthjournals.com/Article/PdfAnnotation>

This PDF needs to be proofread and annotated.

Note: these annotations will not actually change the content of the PDF – they just point out the areas where corrections are needed. The actual corrections will be made to the native article files.

1. **Insert Text Tool:** Text needs inserted into this sentence.
2. **Replace Text Tool:** Some of the text in this paragraph needs to be replaced.
3. **Delete Text Tool:** Some of the text in this overly long sentence needs to be deleted.
4. **Sticky Note Tool:** This image needs to be reduced:



A
B
C
D

NK Cells Restrain Spontaneous Antitumor CD8⁺ T Cell Priming through PD-1/PD-L1 Interactions with Dendritic Cells

Ximena L. Raffo Iraolagoitia,* Raul G. Spallanzani,* Nicolás I. Torres,* Romina E. Araya,* Andrea Ziblat,* Carolina I. Domaica,* Jessica M. Sierra,* Sol Y. Nuñez,* Florencia Secchiari,* Thomas F. Gajewski,^{†,‡} Norberto W. Zwirner,^{*,‡,§} and Mercedes B. Fuertes^{*,¶}

Despite the classical function of NK cells in the elimination of tumor and of virus-infected cells, evidence for a regulatory role for NK cells has been emerging in different models of autoimmunity, transplantation, and viral infections. However, this role has not been fully explored in the context of a growing tumor. In this article, we show that NK cells can limit spontaneous cross-priming of tumor Ag-specific CD8⁺ T cells, leading to reduced memory responses. After challenge with MC57 cells transduced to express the model Ag SIY (MC57.SIY), NK cell-depleted mice exhibited a significantly higher frequency of SIY-specific CD8⁺ T cells, with enhanced IFN- γ production and cytotoxic capability. Depletion of NK cells resulted in a CD8⁺ T cell population skewed toward an effector memory T phenotype that was associated with enhanced recall responses and delayed tumor growth after a secondary tumor challenge with B16.SIY cells. Dendritic cells (DCs) from NK cell-depleted tumor-bearing mice exhibited a more mature phenotype. Interestingly, tumor-infiltrating and tumor-draining lymph node NK cells displayed an upregulated expression of the inhibitory molecule programmed death ligand 1 that, through interaction with programmed death-1 expressed on DCs, limited DC activation, explaining their reduced ability to induce tumor-specific CD8⁺ T cell priming. Our results suggest that NK cells can, in certain contexts, have an inhibitory effect on antitumor immunity, a finding with implications for immunotherapy in the clinic. *The Journal of Immunology*, 2016, 197: 000–000.

Natural killer cells are important mediators of the innate immune response against intracellular pathogens and tumors (1, 2). The recognition of target cells is mediated by a complex repertoire of activating and inhibitory receptors

allowing for the discrimination between normal and infected/transformed cells. An extra level of regulation of NK cell activation is provided by diverse cytokines (3, 4) and the recognition of pathogen-associated molecular patterns through TLRs (5). NK cell activation results not only in a cytotoxic response toward target cells, but also in the secretion of IFN- γ and other cytokines and chemokines (6–8), rendering NK cells capable of modulating the activity of other cells of the immune system and the outcome of the immune response (9–11).

Although it has been widely demonstrated in various model systems that NK cells can play a positive role during immune responses against tumors and infected cells, evidence of an inhibitory role for NK cells is beginning to emerge in diverse models of viral infection (12–15), transplantation (16), and autoimmunity (17). It has been reported that NK cells regulate T cell responses through multiple direct and indirect mechanisms, including NK cell-mediated killing of activated CD8⁺ T cells (14, 15, 18–21), CD4⁺ T cells (18, 19, 22, 23), and also of dendritic cells (DCs) (12, 24, 25). However, little is known about a possible NK cell-mediated inhibitory/regulatory role during antitumor immune responses.

In many instances, spontaneous priming of tumor Ag-specific CD8⁺ T cells can occur in both human cancer patients and in murine models, through DC-mediated cross-presentation. Moreover, a growing body of evidence suggests that an inflamed tumor microenvironment that includes the presence of tumor-infiltrating CD8⁺ T cells has a positive prognostic role in multiple cancer types (26). However, multiple regulatory mechanisms that blunt T cell function within the tumor microenvironment arise in tumors (27). Programmed death ligand 1 (PD-L1), an inhibitory molecule frequently upregulated on tumor cells, is one of the major im-

*Laboratorio de Fisiopatología de la Inmunidad Innata, Instituto de Biología y Medicina Experimental, Consejo Nacional de Investigaciones Científicas y Técnicas, Ciudad de Buenos Aires C1428ADN, Argentina; [†]Section of Hematology/Oncology, Department of Pathology, The University of Chicago, Chicago, IL 60637; [‡]Section of Hematology/Oncology, Department of Medicine, The University of Chicago, Chicago, IL 60637; [§]Departamento de Microbiología, Parasitología e Inmunología, Facultad de Medicina, Universidad de Buenos Aires, Ciudad de Buenos Aires C1121ABG, Argentina; and [¶]Departamento de Química Biológica, Facultad de Ciencias Exactas y Naturales, Universidad de Buenos Aires, Buenos Aires C1428EGA, Argentina

ORCID: 0000-0002-8891-4821 (X.L.R.I.); 0000-0001-5402-3687 (R.G.S.); 0000-0001-9787-2670 (R.E.A.); 0000-0002-7856-2973 (S.Y.N.); 0000-0001-7098-359X (N.W.Z.); 0000-0002-2734-1468 (M.B.F.).

Received for publication October 27, 2015. Accepted for publication May 27, 2016.

This work was supported by grants from the National Agency for Promotion of Science and Technology from Argentina and the National Research Council of Argentina (CONICET) (to M.B.F. and N.W.Z.). X.L.R.I., R.G.S., N.I.T., A.Z., R.E.A., F.S., and S.Y.N. are fellows of CONICET. J.M.S. is a fellow of the Instituto Nacional del Cancer. C.I.D., M.B.F., and N.W.Z. are members of the Researcher Career of CONICET.

Address correspondence and reprint requests to Dr. Norberto W. Zwirner, Laboratorio de Fisiopatología de la Inmunidad Innata, Instituto de Biología y Medicina Experimental, Consejo Nacional de Investigaciones Científicas y Técnicas, Vuelta de Obligado 2490, Ciudad de Buenos Aires C1428ADN, Argentina. E-mail address: nzwirner@ibymc.conicet.gov.ar

The online version of this article contains supplemental material.

Abbreviations used in this article: DC, dendritic cell; IC, isotype control; LN, lymph node; MDSC, myeloid-derived suppressor cell; ND LN, non-draining LN; PD-1, programmed death-1; PD-L1, programmed death-ligand 1; qPCR, quantitative PCR; T_{CM}, central memory T cell; TDLN, tumor-draining LN; T_{EM}, effector memory T cell; TINK, tumor-infiltrating NK; Treg, regulatory T cell.

Copyright © 2016 by The American Association of Immunologists, Inc. 0022-1767/16/\$30.00

munological checkpoints contributing to tumor-immune escape (28) through the inhibition of T cell activation and promotion of apoptosis of DCs (29) and CD8⁺ T cells (30). In several clinical trials, blockade of programmed death-1 (PD-1) or PD-L1 resulted in enhanced T cell function and improved immune-mediated tumor control (31). PD-L1 is expressed not only by tumor cells but also by tumor-infiltrating immune cells (32), and it has been shown that some patients with PD-L1⁻ tumors can also respond to treatment (33). These and other related data have increased the motivation to identify additional regulatory mechanisms that restrain the priming or effector function of tumor-specific T cells.

In this study, we examined the functional role of NK cells during a spontaneous antitumor immune response. We show that NK cells inhibit the expansion of functional tumor-specific CD8⁺ T cells during the priming phase and control the frequency of effector memory T cells (T_{EM}S) CD8⁺ cells, leading to a diminished recall response and reduced tumor control after a secondary tumor challenge with B16.SIY cells. The underlying mechanism involved the regulation of DC maturation, through PD-L1^{hi} NK cells that emerged during tumor growth. Accordingly, NK cell-depleted mice showed an increased frequency of PD-1⁺ DCs. Our results are consistent with a model in which the presence of a growing tumor results in upregulation expression of PD-L1 on NK cells leading to a direct regulation of DC maturation, compromising CD8⁺ T cell priming and recall responses against tumor-derived Ags.

Materials and Methods

Mice

C57BL/6 mice (8–12 wk) were obtained from the animal facility of the School of Veterinary, University of La Plata (Argentina) and housed at the local animal facility according to National Institutes of Health guidelines. Studies have been approved by the institutional review committee.

Tumor cell lines

Mouse cell lines MC57, B16.F10 (henceforth referred to as B16), and YAC1 were obtained from American Type Culture Collection and transduced to express the model antigenic peptide SIYRYGYL (SIY) that is cross-presented to CD8⁺ T cells through H2-K^b (34). Human cell lines (ECC-1, MDA-MB-453, PC3, Caco2, K562, and HeLa) were obtained from American Type Culture Collection. Tumor cell lines were cultured by standard procedures.

Tumor challenge experiments

Mice were s.c. injected on the flank with 2 × 10⁶ tumor cells or PBS (naive mice). After 6 or 11 d, animals were euthanized and peripheral blood (lysed with ACK buffer), spleens, lymph nodes (LNs), and tumors (disrupted with 1 mg/ml collagenase IV [Sigma-Aldrich] in complete DMEM for 30 min at 37°C) were collected. For NK cell transfer experiments, sorted NK cells from naive spleens were inoculated intratumorally 3 d after mice were challenged with MC57.SIY cells, and analyses were performed 6 d after tumor challenge. For recall experiments, on day 110 after primary tumor challenge, mice were s.c. injected with 5 × 10⁶ B16.SIY cells and, the day before and 4 d later, peripheral blood samples were collected. For IFN-γ, CD107a, and tetramer staining, and for the identification/phenotypic of memory T cells, regulatory T cells (Tregs; CD25⁺FoxP3⁺CD4⁺), myeloid-derived suppressor cells (MDSCs; CD11b⁺Gr-1⁺), DCs (CD11c⁺CD3⁻NKp46⁻), and NK cells (NKp46⁺CD3⁻), samples were collected at the indicated time points, and cell suspensions were prepared and analyzed by flow cytometry. For quantitative PCR (qPCR), tumor-draining LNs (TDLNs) and tumors were analyzed 6 d after tumor challenge. For tumor growth experiments, the longest (l) and shortest (d) diameters were measured three times per week, and the tumor volume was calculated as: (l × d²)/2.

Cell depletion

For NK cell depletion, mice were injected i.p. with 100 μg of anti-NK1.1 (PK136; BioXCell) or isotype control (IC; C1.18.4; BioXCell) 1 d before and every 3 d after tumor challenge. For CD8⁺ T cell depletion, 200 μg of anti-CD8 (YTS 169.4, in-house produced) was injected 1 d before tumor

challenge and once per week thereafter. Depletion was confirmed by flow cytometry in blood and tumor samples.

Flow cytometry and cell sorting

Nonspecific staining was blocked with anti-CD16/32 mAb (2.4G2) for mouse samples or with 10% normal mouse serum for human samples. Cells were labeled according to the experiment with the following fluorochrome-coupled Abs: CD3e (17A.2; UCHT1), CD4 (RM4-5), NKp46 (29A1.4), CD49b (DX5), CD56 (N901), CD8 (53-6.7), CD11b (M1/70), CD11c (N418), Gr-1 (RB6.8C5), CD45R (B220, RA3-6B2), CD86 (GL-1), CD44 (IM7), CD127 (A7R34), PD-1 (29F.1A12), PD-L1 (10F.9G2; 29E.2A3), CD25 (PC61), NKG2D (CX5), KLRG1 (2F1), Ly6C (HK1.4), CD27 (LG.3A10) c-Kit (ACK2), CTLA-4 (UC10-4F10-11), CCR7 (4B12), FoxP3 (FJK-16s), and CD107a (ID4B) from Biologend, Tonbo Biosciences, eBioscience, Beckman Coulter, or Immunotools. For tetramer staining, cells were labeled following the manufacturer's instructions with PE-MHC I dexamers (Immudex) consisting of murine H-2K^b complexed to SIY peptide and analyzed in the CD8⁺CD4⁺B220⁻ population. In some experiments, 5000 beads (Spherotech) were added for quantification purposes. Cell viability was determined with Zombie Green (Biolegend). Samples were acquired in a FACSCanto II-plus flow cytometer (BD Biosciences), and data analysis was conducted with FlowJo software (Tree Star). For cell sorting, spleen cells from naive mice and tumor cells were stained with lineage-specific mAbs for NK cells (CD3⁻CD49b⁺ cells), DCs (CD3⁻CD49b⁻CD11c⁺B220⁻ cells), or CD8⁺ T cells (CD3⁺CD8⁺ cells) and sorted in a FACSARIA II-plus cell sorter (BD Biosciences).

CD8⁺ T cell-mediated IFN-γ production

Six days after tumor challenge, 2 × 10⁵ cells were cultured overnight at 37°C in the presence or absence of the SIY peptide (10 μM). During the last 6 h, Golgi-Plug/Golgi-Stop reagents were added; cells were harvested and stained with anti-CD8, anti-CD4, and anti-B220 mAbs, fixed with 1% paraformaldehyde, permeabilized with Perm Buffer II (BD), stained with anti-IFN-γ mAb, and analyzed by flow cytometry.

CD8⁺ T cell-mediated degranulation

Eleven days after tumor challenge, 10⁵ cells were cultured for 6 h with anti-CD107a mAb and Golgi-Plug/Golgi-Stop reagents (BD), in the absence or in the presence of 10⁵ MC57.SIY cells. Cells were then harvested, stained with anti-CD8, anti-CD4, and anti-B220 mAbs, and analyzed by flow cytometry.

In vitro PD-L1 expression

A total of 1 × 10⁶ splenocytes from naive mice was cultured for 48 h in the absence or in the presence of IL-12 (10 ng/ml; Peprotech), IL-15 (1 ng/ml; Peprotech), and IL-18 (10 ng/ml; MBL), or 1 × 10⁵ MC57 cells, in the presence of blocking mAbs against NKG2D (2.5 μg/ml, 191004; R&D Systems) or IFN-γ (10 μg/ml, XMG1.2; Tonbo) or IC (LTF-2; Tonbo). Cells were harvested, stained with anti-CD3, anti-NKp46, and anti-PD-L1 mAbs, and analyzed by flow cytometry.

PBMCs were isolated from healthy human volunteers (provided by the Service of Transfusion Medicine of the Hospital Churrucavisca, Buenos Aires, Argentina) by Ficoll-Paque Plus (GE Life Sciences) gradient centrifugation, and cultured (5 × 10⁵ cells/well) with the different human cell lines (2 × 10⁵ cells/well) for 48 h. Cells were then harvested and stained with anti-CD3, anti-CD56, and anti-PD-L1 mAbs. Studies have been approved by the institutional review committee of the Instituto de Biología y Medicina Experimental.

Quantitative real-time RT-PCR

Total RNA was obtained and cDNA was synthesized as described previously (35). For qPCR, the SYBR Green PCR Master Mix (Applied Biosystems) was used with the CFX96 Real-Time PCR System (Bio-Rad). Primers were as follows: IL-10 (forward: 5'-TGCTAACCCAGCTCTTAATG-CAGGAC-3', reverse: 5'-CCTTGATTCTGGGCCATGCTTCTC-3'), TGF-β (forward: 5'-AATTCCTGGCGTTACCTTGG-3', reverse: 5'-ATCGAAAGCCCTGTATTCCG-3'), and GAPDH (forward: 5'-CAGAA-CATCATCCCTGCAT-3', reverse: 5'-GTTCAAGCTCTGGGATGACCTT-3'). For IFN-β, primer and probe sets from TaqMan Gene Expression Assays (Applied Biosystems) and TaqMan-based quantification were used. Results were expressed as 2^{-ΔCt} using GAPDH as endogenous control.

DC maturation assay

DC and NK cells from naive spleens and NK cells from tumors were sorted. DCs (5 × 10⁴ cells/well) were stimulated with LPS (25 ng/ml; Invivogen)

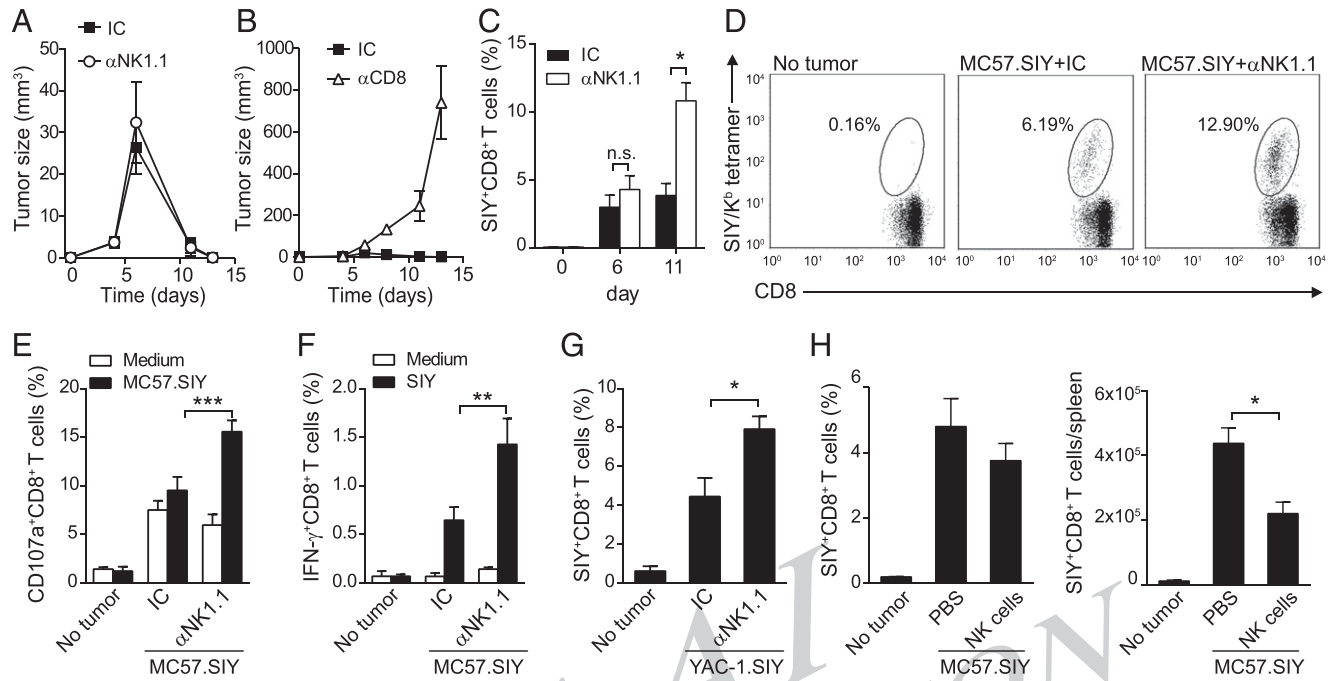


FIGURE 1. NK cell depletion enhances tumor-specific CD8⁺ T cell priming. **(A)** Control (IC) or NK cell-depleted (anti-NK1.1) mice and **(B)** control or CD8⁺ T cell-depleted (anti-CD8) mice were inoculated s.c. with MC57.SIY cells on the flank, and tumor size was evaluated every 2–3 d. **(C–F)** IC or anti-NK1.1-treated mice were inoculated with MC57.SIY cells or left unchallenged (no tumor), and blood was collected at the indicated time points after tumor challenge. **(C)** Percentage of SIY⁺ CD8⁺ T cells assessed by flow cytometry using specific tetramers. **(D)** Representative dot plots of SIY-tetramer staining at day 11. Numbers indicate percent of cells within the indicated gate. **(E)** Percentage of CD107a⁺ CD8⁺ T cells after ex vivo restimulation with MC57.SIY cells or medium. **(F)** Percentage of IFN- γ -producing CD8⁺ T cells after restimulation with soluble SIY peptide or medium. **(G)** Control or NK cell-depleted mice were inoculated with YAC1.SIY cells and blood was collected 11 d later. Percentage of SIY-specific CD8⁺ T cells assessed as in **(C)**. **(H)** Mice were challenged with MC57.SIY cells and 3 d later they received either 7.5×10^4 NK cells intratumorally or PBS. Six days after tumor challenge, splenocytes were harvested. Percentage (*left panel*) and absolute number of SIY-specific CD8⁺ T cells (*right panel*) assessed as in **(C)**. Data represent mean \pm SEM ($n = 4$) and correspond to three (**C**, **E**, and **F**) or two (**A**, **B**, **G**, and **H**) independent experiments. * $p < 0.05$, ** $p < 0.01$, *** $p < 0.001$, two-sided Student t test (**C**, **G**, and **H**) and two-way ANOVA and Tukey multiple comparison test (**E** and **F**).

and R848 (10 μ M; Invivogen) in the absence or in the presence of 5×10^4 naive NK cells or tumor-infiltrating NK (TINK) cells treated or not with anti-PD-L1 blocking mAb (10F.9G2, 10 μ g/ml). After 18 h beads were added and cells were harvested, stained with Zombie Green and for CD11c, CD86, and NKp46, and analyzed by flow cytometry.

T cell proliferation assay

NK cells from naive spleens and from tumors were sorted. T cells isolated from naive spleens by magnetic cell sorting with CD90.2 microbeads (Miltenyi Biotec) were stained with cell proliferation dye eFluor 670 (2.5 μ M; eBioscience). T cells (1×10^5 cells/well) were stimulated with plate-bound anti-CD3 (145-2C11; 2 μ g/ml; BD Pharmingen) and soluble anti-CD28 (37.51, 1 μ g/ml; BD Pharmingen) mAbs in the absence or in the presence of 5×10^4 naive NK cells or TINK cells. After 72 h, cells were harvested, stained with Zombie Green and for CD3, CD8, and NKp46, and eFluor 670 dilution was analyzed by flow cytometry.

Cytotoxicity assay

CD8⁺ T cells (targets) and NK cells (effectors) from naive spleens and tumors were sorted. Tumor-infiltrating CD8⁺ T cells (labeled with 0.25 μ M eFluor 670) and naive CD8⁺ T cells (labeled with 2.5 μ M eFluor 670) were cocultured 1:1 in the absence or in the presence of naive NK cells or TINK cells at different E:T ratios. After 6 h beads were added and cells were harvested, stained with Zombie Green, and analyzed by flow cytometry. Percent specific cytotoxicity was calculated as (100% Zombie Green^{low} cells in the presence of NK cells) – (100% Zombie Green^{low} cells in the absence of NK cells) for each condition.

Statistical methods

Differences between data sets were analyzed with the two-sided Student t test, one-way and two-way ANOVA (Tukey or Sidak multiple comparison tests) using GraphPad Prism Software.

Results

NK cells restrict tumor-induced CD8⁺ T cell priming

To assess the effect of NK cells on the spontaneous priming of tumor Ag-specific CD8⁺ T cells, we analyzed the frequency and effector responses of endogenous SIY-specific CD8⁺ T cells after s.c. implantation of MC57.SIY cells in control or NK cell-depleted mice. MC57.SIY cells naturally express the NKG2D ligand Rae1 and can be recognized and lysed by NK cells (data not shown); however, NK cell depletion did not affect the kinetics of tumor growth (Fig. 1A). In contrast, tumor rejection is completely dependent on CD8⁺ T cells (Fig. 1B). We observed that 6 d after tumor challenge it was possible to detect an expansion of SIY-specific CD8⁺ T cells in control and NK cell-depleted mice. However, by day 11, mice depleted of NK cells displayed a statistically significant increase in the frequency of SIY-specific CD8⁺ T cells in blood (Fig. 1C, 1D) and spleens (data not shown) compared with nondepleted mice. Such an increased frequency mirrored a heightened ability of these CD8⁺ T cells to degranulate in response to restimulation with MC57.SIY cells (Fig. 1E) and was also accompanied by an increased percentage of IFN- γ -producing CD8⁺ T cells upon restimulation with the SIY Ag (Fig. 1F). These findings were validated using the MHC class I⁺ cell line YAC1.SIY where tumor-specific CD8⁺ T cell responses are entirely dependent on cross-priming and are rejected in an NK cell-dependent manner. Similarly, we observed a statistically significant increase in frequency of SIY-specific CD8⁺ T cells 11 d after tumor challenge in NK cell-depleted versus control-treated mice (Fig. 1G). As a complementary approach, NK

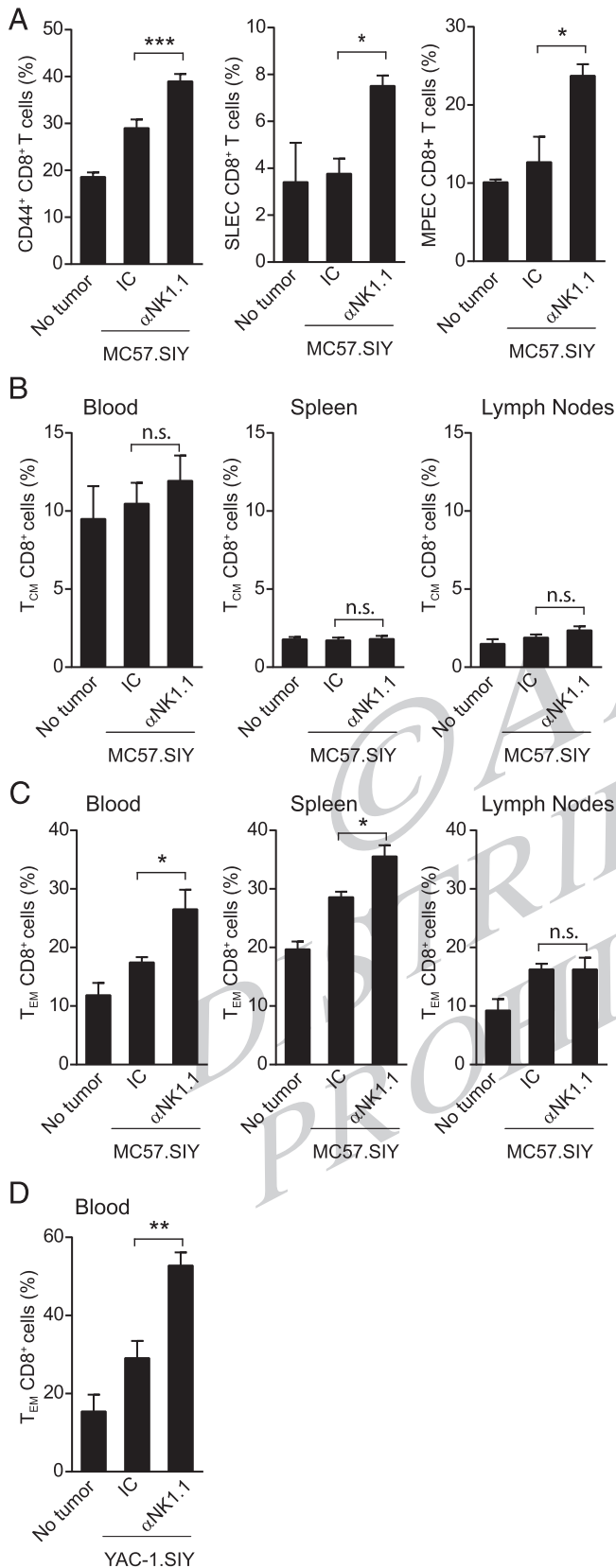


FIGURE 2. NK cell depletion induces the expansion of the T_{EM} CD8⁺ subset. **(A–C)** IC or anti-NK1.1-treated mice were inoculated with MC57.SIY cells; blood, spleen, and LNs were collected. The percentage of CD44⁺, short-lived effector cells and memory precursor effector cells in the CD8⁺ T cell population was evaluated in blood (A), and the percentage of T_{CM} S (B) and T_{EM} S (C) was evaluated by flow cytometry in the CD8⁺ T cell population in blood, spleen, and LNs. **(D)** IC or anti-NK1.1-treated

cells were adoptively transferred intratumorally, which resulted in a reduction in the percentage and number of SIY-specific CD8⁺ T cells (Fig. 1H) and IFN- γ -producing CD8⁺ T cells upon stimulation with SIY peptide (data not shown). These results demonstrate that NK cells can control the expansion of functional Ag-specific CD8⁺ T cells during the priming phase of a spontaneous antitumor immune response.

NK cells restrict the generation of T_{EM} CD8⁺ cells and recall responses to tumors

To further study the role of NK cells on the outcome of tumor-specific CD8⁺ T cell compartment, we characterized the phenotype of effector CD8⁺ T cells primed in control or NK cell-depleted mice based on the expression of CD44, KLRG1, and CD127 markers (36). Mice primed in the absence of NK cells show an augmented proportion of activated CD8⁺ T cells (CD44⁺) including both short-lived effector cells (KLRG1⁺CD127⁻CD44⁺CD8⁺) and memory precursor effector cells (KLRG1⁻CD127⁺CD44⁺CD8⁺) (Fig. 2A). In turn, memory T cells can be divided into two major subtypes: central memory T cells (T_{CM} S) (CD44⁺CD62L^{hi}/CCR7^{hi}) that have little or no effector function but readily proliferate and differentiate to effector cells in response to antigenic stimulation, and T_{EM} S (CD44⁺CD62L^{lo}/CCR7^{lo}) that are widely distributed and display immediate effector functions (37). Although we observed no difference in the T_{CM} CD8⁺ cell population (Fig. 2B), we found a marked increase in the proportion of T_{EM} CD8⁺ subset in spleens and blood of NK cell-depleted mice compared with control mice (Fig. 2C), whereas there was no difference in T_{CM} S and T_{EM} CD4⁺ cells between both groups of mice in blood, spleen, or TDLNs (data not shown). Using the YAC1.SIY model, we recapitulated the results obtained with MC57.SIY (Fig. 2D). These results indicate that NK cell depletion generates a CD8⁺ T cell population skewed toward a T_{EM} phenotype in tumor-bearing mice.

Given these differences, we examined whether the expanded T_{EM} CD8⁺ cell population generated in the absence of NK cells can elicit enhanced recall responses. We challenged NK cell-depleted or control mice with MC57.SIY cells as described earlier, maintaining the NK cell-depleted mice only during the priming phase, and 110 d later (when NK cell counts were normal and tumors were rejected in both groups of mice), we rechallenged mice with the unrelated and poorly immunogenic B16 melanoma, also transduced to express the SIY Ag (B16.SIY) to monitor for SIY-specific memory responses (Fig. 3A). As control, a group of naive mice (that had not been previously injected with MC57.SIY cells) was also challenged with B16.SIY cells. One day before and 4 d after rechallenge we analyzed the frequency of SIY⁺CD8⁺ T cells in the blood of the three groups of mice. Mice that had been primed in the absence of NK cells retained an expanded T_{EM} CD8⁺ cell population before the second challenge (Fig. 3B) and showed an augmented proportion of Ag-specific CD8⁺ T cells during the recall response (Fig. 3C) and an increased proportion of IFN- γ -producing CD8⁺ T cells when restimulated ex vivo with the SIY Ag (Fig. 3D). Priming with MC57.SIY cells induced a strong memory response in mice rechallenged with B16.SIY cells. In addition, if priming occurred in the absence of NK cells, it resulted in delayed tumor growth among mice that did not reject

mice were inoculated with YAC1.SIY cells, blood was collected 11 d later, and the percentage of T_{EM} CD8⁺ cells was evaluated by flow cytometry. Data represent mean \pm SEM ($n = 4$) and correspond to two independent experiments. * $p < 0.05$, ** $p < 0.01$, *** $p < 0.001$, two-sided Student t test. n.s., not significant.

the tumor (Fig. 3E) and a trend toward enhanced protection against secondary tumor formation (Fig. 3F, tumor development in 11.11% of anti-NK1.1-treated mice versus 31.25% of IC-treated mice). These results indicate that the NK cell-dependent shaping of the memory compartment during the first tumor challenge may result in diminished recall responses and poor tumor control.

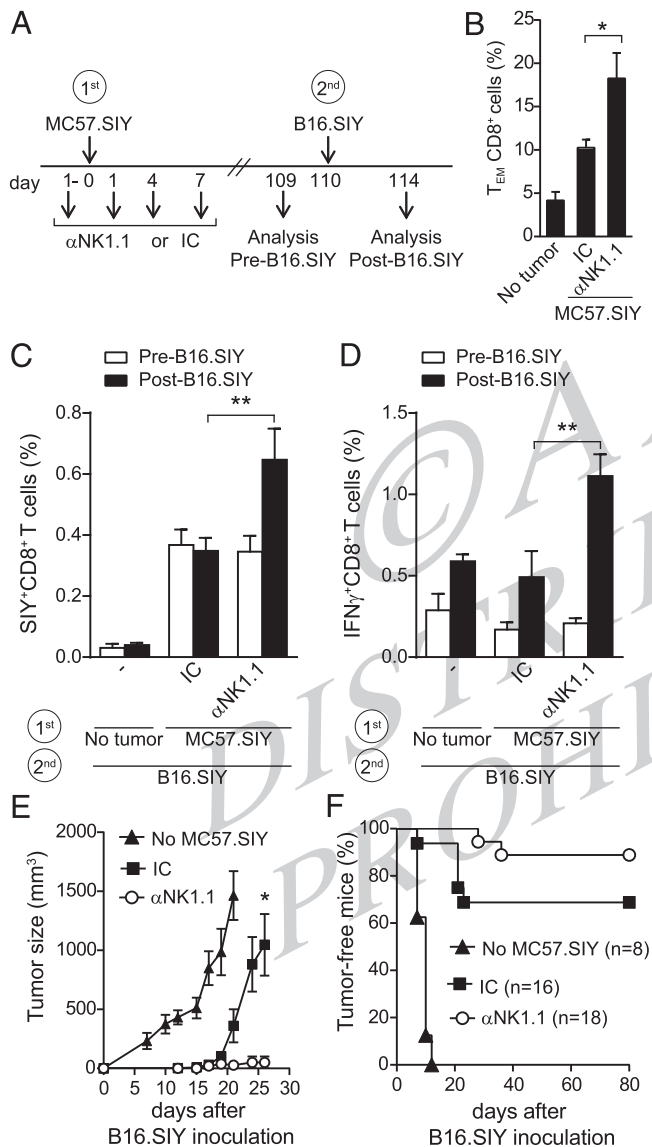


FIGURE 3. NK cell depletion during priming enhances antitumor recall responses. IC or anti-NK1.1-treated mice were inoculated with MC57.SIY cells (first challenge) or left unchallenged (no tumor). After 110 d, mice were challenged with B16.SIY cells (second challenge); 1 d before (pre-B16.SIY) and 4 d later (post-B16.SIY), blood was collected and analyzed. (A) Experimental design. (B) Percentage of T_{EM} CD8⁺ cells 109 d after challenge with MC57.SIY (pre-B16.SIY). (C) Percentage of SIY-specific CD8⁺ T cells. (D) Percentage of IFN-γ-producing CD8⁺ T cells after restimulation with soluble SIY peptide. Data represent mean ± SEM (*n* = 5) and correspond to two independent experiments. (E) Tumor size (in mice that did not reject the tumor) after challenge with B16.SIY in the three groups of mice and (F) percentage of tumor-free mice (*n* represents the total number of mice analyzed for each group of mice). Data represent mean ± SEM. **p* < 0.05 two-sided Student *t* test, ***p* < 0.01 two-way ANOVA and Tukey multiple comparison test.

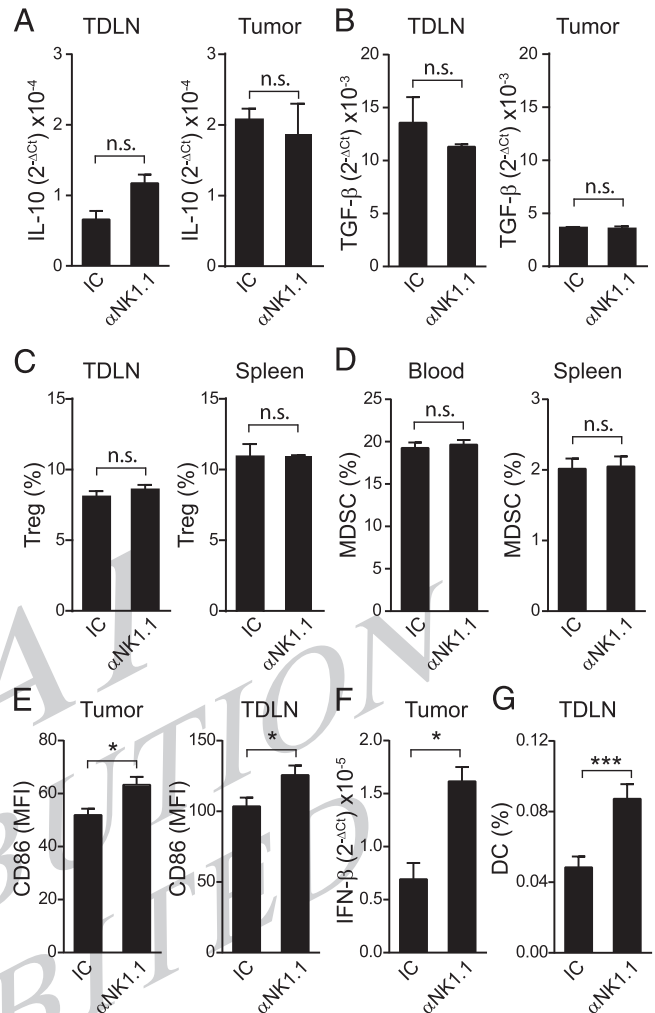


FIGURE 4. NK cell depletion augments DC maturation without affecting other major regulatory populations. IC or anti-NK1.1-treated mice were inoculated with MC57.SIY cells. (A and B) Six days later, TDLNs and tumors were collected and the relative abundance of IL-10 (A) and TGF-β (B) transcripts were evaluated by qPCR. (C and D) Eleven days after tumor inoculation, TDLNs, spleens, and blood were collected and the percentage of Tregs (C) and MDSCs (D) were evaluated by flow cytometry. (E–G) Six days after tumor challenge, tumors and TDLNs were collected and the expression of CD86 on DCs (defined as CD3[−]NKp46[−]B220[−]CD11c⁺) was evaluated by flow cytometry (E), the relative abundance of IFN-β transcripts was evaluated by qPCR (F), and the frequency of DCs was evaluated by flow cytometry. Data represent mean ± SEM (*n* = 3) and correspond to two independent experiments. **p* < 0.05, ****p* < 0.001, two-sided Student *t* test. n.s., not significant.

NK cells limit DC maturation without affecting other regulatory populations

NK cells with regulatory functions, capable of dampening Ag-specific T cell responses through the secretion of the immunosuppressive cytokines IL-10 and/or TGF-β, have been described previously (38). However, when we compared the amounts of IL-10 and TGF-β mRNA in tumors and TDLNs, we found no differences between NK cell-depleted and control mice (Fig. 4A, F, 4B). Although NK cells can recruit Tregs via secretion of the chemokine CCL22, which may contribute to immune suppression (39), we found no differences in the frequency of Tregs in tumor or TDLNs between control and NK cell-depleted mice (Fig. 4C).

MDSCs constitute one of the major populations of immune cells capable of regulating antitumor immune responses (40). In addi-

538
539
540
541
542
543
544
545
546
547
548
549
550
551
552
553
554
555
556
557
558
559
560
561
562
563
564
565
566
567
568
569
570
571
572
573
574
575
576
577
578
579
580
581
582
583
584
585
586
587
588
589
590
591
592
593
594
595
596
597
598
599
600
601

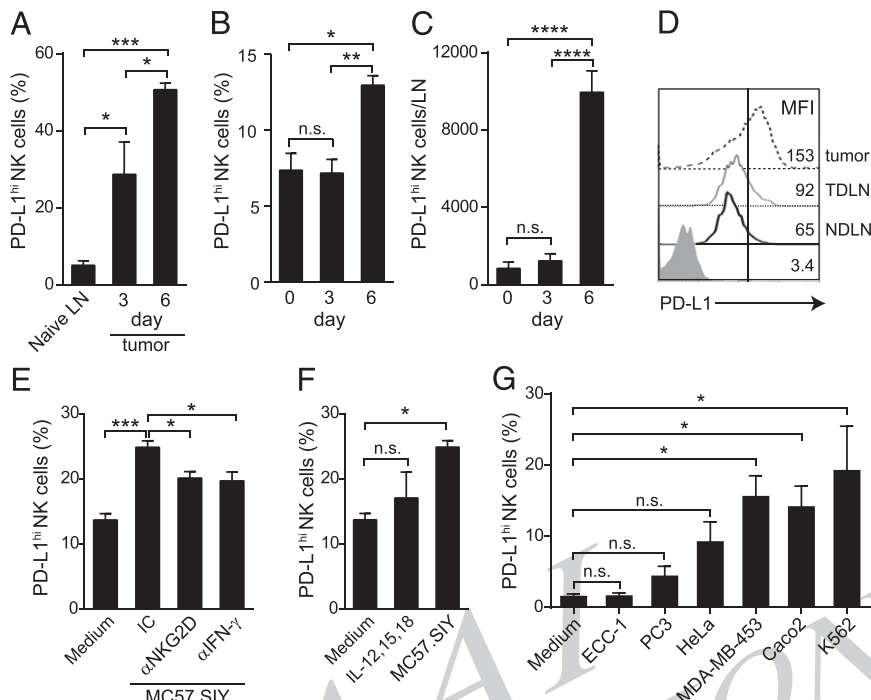


FIGURE 5. Tumors induce PD-L1 expression on NK cells. (A–D) Mice were inoculated with MC57.SIY cells, and 3 and 6 d later, tumors, TDLNs, NDLNs, and naive LNs were collected and the expression of PD-L1 was analyzed by flow cytometry on NK cells (defined as CD3⁺NKp46⁺ cells). (A) Percentage of PD-L1^{hi} NK cells in naive LNs and tumors. (B) Percentage and (C) number of PD-L1^{hi} NK cells in TDLNs on days 0, 3, and 6 after tumor challenge. (D) Representative histograms of PD-L1 expression on NK cells in tumors, TDLNs, and NDLNs. The filled histogram corresponds to the IC. (A–C) Data represent mean ± SEM ($n = 4$) and correspond to two independent experiments. (E and F) A total of 10^6 splenocytes were cultured with 10^5 MC57.SIY in the presence of IC, anti-IFN- γ neutralizing mAb, or anti-NKG2D blocking mAb (E), or in the presence of IL-12, IL-15, and IL-18 or 10^5 MC57.SIY (F), and after 48 h, the percentage of PD-L1^{hi} NK cells was analyzed by flow cytometry. (E and F) Data represent mean ± SEM ($n = 4$) and correspond to two independent experiments. (G) Human PBMCs were cultured with the indicated tumor cell lines, and 48 h later the percentage of PD-L1^{hi} NK cells (defined as CD3⁺CD56⁺ cells) was evaluated by flow cytometry. Data represent mean ± SEM ($n = 4$ donors). * $p < 0.05$, ** $p < 0.01$, *** $p < 0.001$, two-sided Student t test (A–C) and one-way ANOVA and Tukey multiple comparison test (E–G). MFI, mean fluorescence intensity.

tion, it has recently been described that CD11b⁺CD27⁺ NK cells could be converted into CD11b⁺Gr1⁺ MDSCs in tumor-bearing mice (41). However, when we compared the proportion of MDSCs in blood and spleens of NK cell-depleted or control mice, we found no differences (Fig. 4D).

The striking difference for CD8⁺ T cell priming observed upon NK cell depletion could point to a defect at the level of DC costimulation and cross-priming of CD8⁺ T cells. Therefore, we compared the maturation status of DCs in both groups of mice and found an enhanced expression of CD86 on tumor-infiltrating and TDLN DCs in mice lacking NK cells compared with control mice (Fig. 4E). These observations suggest that NK cells can restrict DC maturation. Considering that IFN- β produced by DCs early during an antitumor immune response is critical for priming of CD8⁺ T cells (42), expression of this cytokine also was examined. In fact, tumors from NK cell-depleted mice showed a 2.33-fold increase in the levels of IFN- β (Fig. 4F). Moreover, we found an elevated frequency of DCs in TDLNs from NK cell-depleted mice compared with control mice (Fig. 4G). Together, these results suggest a regulatory function of NK cells at the level of DCs.

Tumor-experienced NK cells have an altered phenotype and express PD-L1

In a search for possible phenotypic changes on NK cells during antitumor immune responses that could account for their regulatory ability, we assessed the expression of several stage-related and activation/inhibitory markers on NK cells. We found that TINK cells are mostly the terminally differentiated CD11b⁺CD27⁻ subpopulation (43) (Supplemental Fig. 1A). Still, compared with

NK cells from naive LN, TINK cells showed an altered phenotype that included upregulation of KLRG1 (capable of inhibiting NK cell effector functions [44]), Ly6C (associated with an inert state [45]), and CD25 (Supplemental Fig. 1B), the downregulation of activating receptors NKG2D and NKp46 (Supplemental Fig. 1C), and no change in the potentially inhibitory molecules PD-1, CTLA-4 (46), and c-Kit (Supplemental Fig. 1D). The PD-1/PD-L1 pathway is one of the most critical checkpoints responsible for mediating tumor-induced immune suppression (33). Notably, 6 d after tumor inoculation, we observed an expansion in the frequency and numbers of PD-L1-expressing NK cells (PD-L1^{hi} NK cells), not only in tumors (Fig. 5A) but also in TDLNs compared with naive or non-draining LNs (NDLNs; Fig. 5B–D). To evaluate whether this phenotypic change could be mediated by interaction with tumor cells, we cocultured splenocytes with MC57 tumor cells in vitro. Indeed, this resulted in a 2-fold expansion of PD-L1^{hi} NK cells (Fig. 5E). This effect was dependent on IFN- γ , and the activating NK cell receptor NKG2D as neutralization of IFN- γ or blockade of NKG2D during the coculture of splenocytes with MC57 cells partially inhibited the upregulation of PD-L1 (Fig. 5E). In contrast with this tumor-induced phenotypic change, no increase in PD-L1-expressing NK cells was observed upon stimulation with the cytokines IL-12, IL-15, and IL-18 (Fig. 5F). In addition, human NK cells also upregulated PD-L1 expression after tumor recognition in vitro (Fig. 5G), indicating that certain tumors can induce the upregulation of PD-L1 on both mouse and human NK cells.

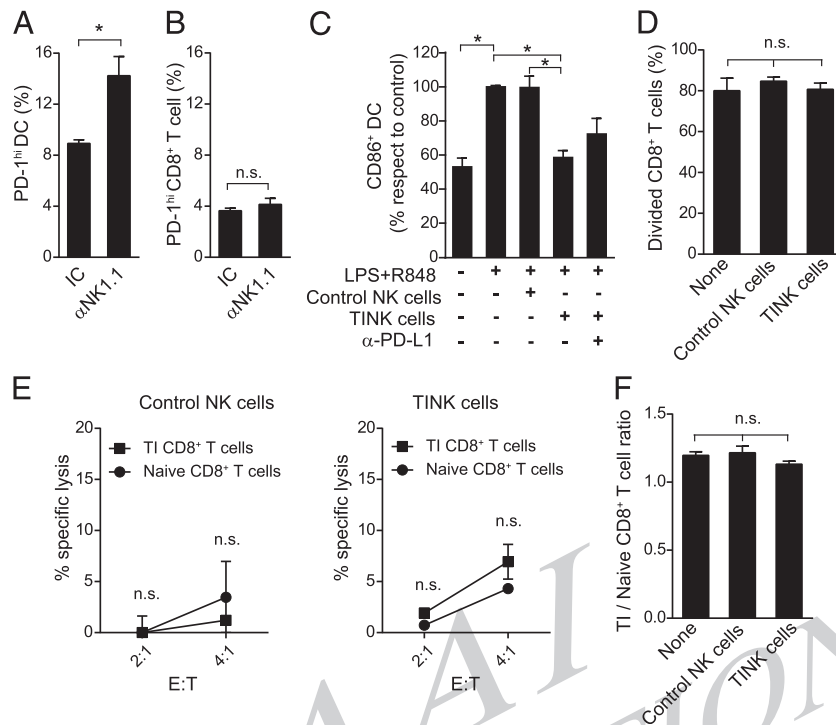


FIGURE 6. NK cells negatively regulate DC maturation through PD-1/PD-L1 interactions. (A and B) IC or anti-NK1.1–treated mice were inoculated with MC57.SIY cells, and 6 d later PD-1 expression was evaluated by flow cytometry in DCs (A) and CD8⁺ T cells (B) from TDLNs. (C) Sorted splenic DCs were stimulated with LPS and R848 (control) in the absence or in the presence of control NK cells (isolated from spleen of naive mice) or TINK cells, in the absence or in the presence of an anti-PD-L1 blocking mAb, and 18 h later the number of viable mature DCs (defined as CD11c⁺CD86⁺Zombie Green⁻ cells and depicted as percentage of the control) was evaluated by flow cytometry. (D) eFluor 670–labeled CD3⁺ T cells were stimulated with anti-CD3/anti-CD28 and cultured in the absence or in the presence of control NK cells or TINK cells, and 72 h later the percentage of divided CD8⁺ T cells was evaluated by flow cytometry. (E and F) eFluor 670–labeled naive (eFluor 670^{high}) and tumor-infiltrating (TI; eFluor 670^{low}) CD8⁺ T cells were cultured in the absence or in the presence of control NK or TINK cells, and 6 h later the percentage of nonviable CD8⁺ T cells (100-Zombie Green⁻ cells) was evaluated by flow cytometry and % specific cytotoxicity (E), and the viable TI/Naive CD8⁺ T cell ratio (F) was calculated (E:T = 4:1). Data represent mean ± SEM [(A and B) *n* = 4; (C–F) *n* = 2] and correspond to two independent experiments. **p* < 0.05, two-sided Student *t* test (A and B), one-way ANOVA and Tukey (C, D, and F), or Sidak (E) multiple comparison test. n.s., not significant.

NK cells regulate DC maturation through PD-1/PD-L1 interactions

We wondered whether increased expression of PD-L1 on NK cells might contribute to the diminished priming of CD8 T cells observed in tumor-bearing mice, through targeting DCs and/or CD8⁺ T cells. Therefore, we first analyzed whether NK cells might control DC and CD8⁺ T cell numbers in a PD-1/PD-L1–dependent manner in vivo. Mice depleted of NK cells exhibited a 1.6-fold increase in the frequency of PD-1^{hi} DCs (Fig. 6A) but showed no difference in PD-1–expressing CD8⁺ T cells (Fig. 6B) compared with control mice. Accordingly, in vitro DC maturation with LPS and R848 was inhibited in the presence of TINK cells but not in the presence of NK cells from a naive spleen, and this inhibition was partially reverted by blockade of PD-L1 (Fig. 6C). To explore a potential direct effect of PD-L1^{hi} NK cells on CD8⁺ T cells, we analyzed the proliferation and survival of activated CD8⁺ T cells in the presence of TINK cells. We found that in vitro proliferation of these CD8⁺ T cells (that uniformly expressed high levels of PD-1, data not shown) was not altered in the presence of control (isolated from naive spleens) or tumor-derived NK cells (Fig. 6D). In addition, naive and tumor-infiltrating CD8⁺ T cells were equally resistant to NK cell–mediated lysis (Fig. 6E), either when we used control NK cells or PD-L1^{hi} TINK cells as effectors (Fig. 6F). These results indicate that TINK cells were unable to directly suppress CD8⁺ T cell proliferation or to preferentially kill tumor-infiltrating CD8⁺ T cells, but that they can regulate the maturation

status of DCs, in part through PD-1/PD-L1 interactions, and in such manner indirectly affect CD8⁺ T cell priming.

Discussion

Evidence supporting a regulatory role for NK cells in diverse immunopathological conditions such as viral infections, autoimmunity, and transplantation is emerging (12–17). However, little is known about a possible regulatory activity during an antitumor immune response. In this study, we took advantage of the SIY model Ag to track the priming of endogenous tumor-specific CD8⁺ T cells in vivo in the presence or in the absence of NK cells. We show that NK cells can control the spontaneous priming and memory responses of tumor Ag-specific CD8⁺ T cells, in part through a mechanism involving regulation of DC maturation through PD-1/PD-L1 interaction.

Despite the enhanced priming of tumor-specific CD8⁺ T cells in NK cell–depleted mice, the primary tumor is equally rejected by control mice. This is due to the high immunogenicity of MC57.SIY cells, which induce substantial amounts of tumor-specific CD8⁺ T cells, high enough to induce tumor rejection simultaneously or before the regulatory activity of NK cells becomes apparent.

In vivo, the absence of NK cells resulted in enhanced priming of antitumor CD8⁺ T cells and a memory response skewed toward a T_{EM} phenotype that led to a faster and more robust recall response resulting in delayed tumor growth. These results may have implications for the rational design of cancer immunotherapies given

that the induction of durable antitumor T cell responses in cancer patients is a major goal of therapeutic interventions (26).

The regulatory role described in this article for NK cells is in sharp contrast with its well-known role in the control of tumor growth and infectious agents. This apparent contradiction may reflect the complex and yet incompletely understood biology of NK cells, which when faced with different stimuli might generate alternative outcomes at different stages of the immune response. In the tumor context, Schreiber and colleagues (47) showed that, although NK cells could play a critical role during the elimination of tumor cells, during the equilibrium (dormancy phase) of an antitumor immune response, NK cells seem to be expendable. In our model, PD-L1^{hi} NK cells become detectable in TDLNs 6 d after tumor challenge, consistent with the idea that NK cells can be functional and contribute to tumor control early after tumor challenge and become suppressive later on.

Such a regulatory activity of NK cells at the level of the adaptive immune response may have evolved as a mechanism to control the extent of T cell activation in the context of chronic viral infections and other immune pathological conditions, to limit damage that can be associated with widespread T cell responses. Accordingly, some patients with autoimmune disorders display reduced NK cell numbers with impaired cytotoxicity (48).

PD-L1 is a powerful immune modulator differentially expressed during tumor progression on tumor cells, stroma, or immune cells that contributes to immune escape. Blocking agents targeting this pathway are currently being tested with promising results in clinical trials, including FDA approval in both melanoma and lung cancer (49). In this article, we show that, consistent with a regulatory function of NK cells, PD-L1 was overexpressed by NK cells from tumor-bearing mice, and that induction of PD-L1 expression was dependent on NKG2D recognition. PD-L1 was also upregulated on human NK cells upon coculture with some but not all of the human cell lines tested. However, there was no correlation between NKG2D ligand expression and PD-L1 upregulation, suggesting that other activating/inhibiting receptors might be involved. It has been shown that IFN- γ is a positive regulator for PD-L1 expression (50). Accordingly, we observed that blockade of IFN- γ prevented the generation of PD-L1^{hi} NK cells. Although we cannot rule out the possibility that NK cell-derived IFN- γ might also trigger PD-L1 upregulation on stroma or other immune cells that may partially contribute to the regulation of the immune response, we found no difference between NK cell-depleted and control mice when analyzing PD-L1 expression on tumor cells in vivo (data not shown).

The observed PD-L1 expression on NK cells has functional consequences, because tumor-experienced NK cells controlled DC maturation in vivo and in vitro, and PD-L1 blockade partially restored the numbers of mature DCs recovered in vitro. Accordingly, we found an expanded population of PD-1^{hi} DCs in TDLNs of NK cell-depleted mice compared with control mice. Conversely, PD-L1^{hi} NK cells were unable to kill CD8⁺ T cells or to directly suppress its proliferation in vitro. Moreover, in vivo, the frequency of PD-1^{hi} CD8⁺ T cells was unchanged in the presence or in the absence of NK cells.

PD-L1 expression on c-Kit⁺CD11b⁻ NK cells during experimental diabetes (17) and metastatic spread of cancer (51) has been reported. However, in our experimental setting, we observed that PD-L1^{hi} NK cells showed no detectable expression of c-Kit and were mostly terminally differentiated, expressing high levels of CD11b.

PD-L1 expression on tumor cells is a suggestive, but inadequate, predictive biomarker of response to immune-checkpoint blockade (31), suggesting that PD-L1 expressed by other cells might also be

a relevant target for therapy with these agents. It is conceivable that the blockade of PD-L1 on NK cells could be part of the mechanism of action of these Abs, through disruption of the regulatory interaction between NK cells and DCs, which could contribute to the more robust and efficient antitumor CD8⁺ T cell response seen with anti-PD-1.

In summary, our results suggest a model in which tumor-induced PD-L1^{hi} NK cells regulate DC activation resulting in a reduced ability to support CD8⁺ T cell priming. The assessment of PD-L1 expression on NK cells should be investigated as a potential biomarker for the presence of regulatory NK cells and also in association with clinical outcomes with anti-PD-1 mAbs. Q:13

Acknowledgments

We thank Dr. Gabriel A. Rabinovich (Laboratory of Immunopathology, Instituto de Biología y Medicina Experimental) for continuous support and for generously providing unlimited access to the Flow Cytometry and Cell Sorting Facility and Fundación René Barón for providing additional support. Q:14

Disclosures

The authors have no financial conflicts of interest.

References

- Lanier, L. L. 2008. Evolutionary struggles between NK cells and viruses. *Nat. Rev. Immunol.* 8: 259–268.
- Moretta, L., C. Bottino, D. Pende, R. Castriconi, M. C. Mingari, and A. Moretta. 2006. Surface NK receptors and their ligands on tumor cells. *Semin. Immunol.* 18: 151–158.
- Zwimer, N. W., and C. I. Domaica. 2010. Cytokine regulation of natural killer cell effector functions. *Biofactors* 36: 274–288.
- Ziblat, A., C. I. Domaica, R. G. Spallanzani, X. L. Iraolagoitia, L. E. Rossi, D. E. Avila, N. I. Torres, M. B. Fuertes, and N. W. Zwimer. 2015. IL-27 stimulates human NK-cell effector functions and primes NK cells for IL-18 responsiveness. *Eur. J. Immunol.* 45: 192–202.
- Girart, M. V., M. B. Fuertes, C. I. Domaica, L. E. Rossi, and N. W. Zwimer. 2007. Engagement of TLR3, TLR7, and NKG2D regulate IFN-gamma secretion but not NKG2D-mediated cytotoxicity by human NK cells stimulated with suboptimal doses of IL-12. *J. Immunol.* 179: 3472–3479.
- Lanier, L. L. 2008. Up on the tightrope: natural killer cell activation and inhibition. *Nat. Immunol.* 9: 495–502.
- Vivier, E., E. Tomasello, M. Baratin, T. Walzer, and S. Ugolini. 2008. Functions of natural killer cells. *Nat. Immunol.* 9: 503–510.
- Vivier, E., D. H. Raulet, A. Moretta, M. A. Caligiuri, L. Zitvogel, L. L. Lanier, W. M. Yokoyama, and S. Ugolini. 2011. Innate or adaptive immunity? The example of natural killer cells. *Science* 331: 44–49.
- Moretta, A., E. Marcenaro, S. Sivori, M. Della Chiesa, M. Vitale, and L. Moretta. 2005. Early liaisons between cells of the innate immune system in inflamed peripheral tissues. *Trends Immunol.* 26: 668–675.
- Walzer, T., M. Dalod, S. H. Robbins, L. Zitvogel, and E. Vivier. 2005. Natural-killer cells and dendritic cells: “l’union fait la force”. *Blood* 106: 2252–2258.
- Martín-Fontecha, A., L. L. Thomsen, S. Brett, C. Gerard, M. Lipp, A. Lanzavecchia, and F. Sallusto. 2004. Induced recruitment of NK cells to lymph nodes provides IFN-gamma for T(H)1 priming. *Nat. Immunol.* 5: 1260–1265.
- Cook, K. D., and J. K. Whitmire. 2013. The depletion of NK cells prevents T cell exhaustion to efficiently control disseminating virus infection. *J. Immunol.* 190: 641–649.
- Schuster, I. S., M. E. Wikstrom, G. Brizard, J. D. Coudert, M. J. Estcourt, M. Manzur, L. A. O’Reilly, M. J. Smyth, J. A. Trapani, G. R. Hill, et al. 2014. TRAIL⁺ NK cells control CD4⁺ T cell responses during chronic viral infection to limit autoimmunity. *Immunity* 41: 646–656.
- Lang, P. A., K. S. Lang, H. C. Xu, M. Grusdat, I. A. Parish, M. Recher, A. R. Elford, S. Dhanji, N. Shaabani, C. W. Tran, et al. 2012. Natural killer cell activation enhances immune pathology and promotes chronic infection by limiting CD8⁺ T-cell immunity. *Proc. Natl. Acad. Sci. USA* 109: 1210–1215.
- Waggoner, S. N., R. T. Taniguchi, P. A. Mathew, V. Kumar, and R. M. Welsh. 2010. Absence of mouse 2B4 promotes NK cell-mediated killing of activated CD8⁺ T cells, leading to prolonged viral persistence and altered pathogenesis. *J. Clin. Invest.* 120: 1925–1938.
- Laffont, S., C. Seillet, J. Ortaldo, J. D. Coudert, and J. C. Guéry. 2008. Natural killer cells recruited into lymph nodes inhibit alloreactive T-cell activation through perforin-mediated killing of donor allogeneic dendritic cells. *Blood* 112: 661–671.
- Ehlers, M., C. Papewalis, W. Stenzel, B. Jacobs, K. L. Meyer, R. Deenen, H. S. Willenberg, S. Schinner, A. Thiel, W. A. Scherbaum, et al. 2012. Immunoregulatory natural killer cells suppress autoimmunity by down-regulating antigen-specific CD8⁺ T cells in mice. *Endocrinology* 153: 4367–4379.

- 986 18. Rabinovich, B. A., J. Li, J. Shannon, R. Hurren, J. Chalupny, D. Cosman, and
987 R. G. Miller. 2003. Activated, but not resting, T cells can be recognized and
988 killed by syngeneic NK cells. *J. Immunol.* 170: 3572–3576.
- 989 19. Cerboni, C., A. Zingoni, M. Cippitelli, M. Piccoli, L. Frati, and A. Santoni. 2007.
990 Antigen-activated human T lymphocytes express cell-surface NKG2D ligands
991 via an ATM/ATR-dependent mechanism and become susceptible to autologous
992 NK-cell lysis. *Blood* 110: 606–615.
- 993 20. Soderquest, K., T. Walzer, B. Zafirova, L. S. Klavinskis, B. Polić, E. Vivier,
994 G. M. Lord, and A. Martín-Fontecha. 2011. Cutting edge: CD8+ T cell priming
995 in the absence of NK cells leads to enhanced memory responses. *J. Immunol.*
996 186: 3304–3308.
- 997 21. Peppas, D., U. S. Gill, G. Reynolds, N. J. Easom, L. J. Pallett, A. Schurich,
998 L. Micco, G. Nebbia, H. D. Singh, D. H. Adams, et al. 2013. Up-regulation of a
999 death receptor renders antiviral T cells susceptible to NK cell-mediated deletion.
1000 *J. Exp. Med.* 210: 99–114.
- 1001 22. Lu, L., K. Ikizawa, D. Hu, M. B. Werneck, K. W. Wucherpfennig, and H. Cantor.
1002 2007. Regulation of activated CD4+ T cells by NK cells via the Qa-1-NKG2A
1003 inhibitory pathway. *Immunity* 26: 593–604.
- 1004 23. Waggoner, S. N., M. Cornberg, L. K. Selin, and R. M. Welsh. 2011. Natural
1005 killer cells act as rheostats modulating antiviral T cells. *Nature* 481: 394–398.
- 1006 24. Andrews, D. M., M. J. Estcourt, C. E. Andoniou, M. E. Wikstrom, A. Khong,
1007 V. Voigt, P. Fleming, H. Tabarias, G. R. Hill, R. G. van der Most, et al. 2010.
1008 Innate immunity defines the capacity of antiviral T cells to limit persistent
1009 infection. *J. Exp. Med.* 207: 1333–1343.
- 1010 25. Hayakawa, Y., V. Screpanti, H. Yagita, A. Grandien, H. G. Ljunggren,
1011 M. J. Smyth, and B. J. Chambers. 2004. NK cell TRAIL eliminates immature
1012 dendritic cells in vivo and limits dendritic cell vaccination efficacy. *J. Immunol.*
1013 172: 123–129.
- 1014 26. Gajewski, T. F., H. Schreiber, and Y. X. Fu. 2013. Innate and adaptive immune
1015 cells in the tumor microenvironment. *Nat. Immunol.* 14: 1014–1022.
- 1016 27. Rabinovich, G. A., D. Gabrilovich, and E. M. Sotomayor. 2007. Immunosup-
1017 pressive strategies that are mediated by tumor cells. *Annu. Rev. Immunol.* 25:
1018 267–296.
- 1019 28. Blank, C., T. F. Gajewski, and A. Mackensen. 2005. Interaction of PD-L1 on
1020 tumor cells with PD-1 on tumor-specific T cells as a mechanism of immune
1021 evasion: implications for tumor immunotherapy. *Cancer Immunol. Immunother.*
1022 54: 307–314.
- 1023 29. Park, S. J., H. Namkoong, J. Doh, J. C. Choi, B. G. Yang, Y. Park, and Y. Chul
1024 Sung. 2014. Negative role of inducible PD-1 on survival of activated dendritic
1025 cells. *J. Leukoc. Biol.* 95: 621–629.
- 1026 30. Driessens, G., J. Kline, and T. F. Gajewski. 2009. Costimulatory and coinhibitory
1027 receptors in anti-tumor immunity. *Immunol. Rev.* 229: 126–144.
- 1028 31. Mahoney, K. M., G. J. Freeman, and D. F. McDermott. 2015. The next immu-
1029 ne-checkpoint inhibitors: PD-1/PD-L1 blockade in melanoma. *Clin. Ther.* 37: 764–
1030 782.
- 1031 32. Herbst, R. S., J. C. Soria, M. Kowanetz, G. D. Fine, O. Hamid, M. S. Gordon,
1032 J. A. Sosman, D. F. McDermott, J. D. Powderly, S. N. Gettinger, et al. 2014.
1033 Predictive correlates of response to the anti-PD-L1 antibody MPDL3280A in
1034 cancer patients. *Nature* 515: 563–567.
- 1035 33. Teng, M. W., S. F. Ngiew, A. Ribas, and M. J. Smyth. 2015. Classifying cancers
1036 based on T-cell infiltration and PD-L1. *Cancer Res.* 75: 2139–2145.
- 1037 34. Zhang, B., N. A. Bowerman, J. K. Salama, H. Schmidt, M. T. Spiotto,
1038 A. Schietinger, P. Yu, Y. X. Fu, R. R. Weichselbaum, D. A. Rowley, et al. 2007.
1039 Induced sensitization of tumor stroma leads to eradication of established cancer
1040 by T cells. *J. Exp. Med.* 204: 49–55.
- 1041 35. Rossi, L. E., D. E. Avila, R. G. Spallanzani, A. Ziblat, M. B. Fuentes,
1042 L. Lapyckyj, D. O. Croci, G. A. Rabinovich, C. I. Domaica, and N. W. Zwirner.
1043 2012. Histone deacetylase inhibitors impair NK cell viability and effector
1044 functions through inhibition of activation and receptor expression. *J. Leukoc.*
1045 *Biol.* 91: 321–331.
- 1046 36. Joshi, N. S., W. Cui, A. Chandele, H. K. Lee, D. R. Urso, J. Hagman, L. Gapin,
1047 and S. M. Kaech. 2007. Inflammation directs memory precursor and short-lived
1048 effector CD8(+) T cell fates via the graded expression of T-bet transcription
1049 factor. *Immunity* 27: 281–295.
- 1050 37. Sallusto, F., J. Geginat, and A. Lanzavecchia. 2004. Central memory and effector
1051 memory T cell subsets: function, generation, and maintenance. *Annu. Rev.*
1052 *Immunol.* 22: 745–763.
- 1053 38. Deniz, G., G. Erten, U. C. Küçüksezer, D. Kocacik, C. Karagiannidis, E. Aktas,
1054 C. A. Akdis, and M. Akdis. 2008. Regulatory NK cells suppress antigen-specific
1055 T cell responses. *J. Immunol.* 180: 850–857.
- 1056 39. Mailloux, A. W., and M. R. Young. 2009. NK-dependent increases in CCL22
1057 secretion selectively recruits regulatory T cells to the tumor microenvironment.
1058 *J. Immunol.* 182: 2753–2765.
- 1059 40. Youn, J. I., and D. I. Gabrilovich. 2010. The biology of myeloid-derived sup-
1060 pressor cells: the blessing and the curse of morphological and functional het-
1061 erogeneity. *Eur. J. Immunol.* 40: 2969–2975.
- 1062 41. Park, Y. J., B. Song, Y. S. Kim, E. K. Kim, J. M. Lee, G. E. Lee, J. O. Kim,
1063 Y. J. Kim, W. S. Chang, and C. Y. Kang. 2013. Tumor microenvironmental
1064 conversion of natural killer cells into myeloid-derived suppressor cells. *Cancer*
1065 *Res.* 73: 5669–5681.
- 1066 42. Fuertes, M. B., A. K. Kacha, J. Kline, S. R. Woo, D. M. Kranz, K. M. Murphy,
1067 and T. F. Gajewski. 2011. Host type I IFN signals are required for antitumor CD8
1068 + T cell responses through CD8alpha+ dendritic cells. *J. Exp. Med.* 208: 2005–
1069 2016.
- 1070 43. Chiassone, L., J. Chaix, N. Fuseri, C. Roth, E. Vivier, and T. Walzer. 2009.
1071 Maturation of mouse NK cells is a 4-stage developmental program. *Blood* 113:
1072 5488–5496.
- 1073 44. Robbins, S. H., K. B. Nguyen, N. Takahashi, T. Mikayama, C. A. Biron, and
1074 L. Brossay. 2002. Cutting edge: inhibitory functions of the killer cell lectin-like
1075 receptor G1 molecule during the activation of mouse NK cells. *J. Immunol.* 168:
1076 2585–2589.
- 1077 45. Omi, A., Y. Enomoto, T. Kuniwa, N. Miyata, and A. Miyajima. 2014. Mature
1078 resting Ly6C(high) natural killer cells can be reactivated by IL-15. *Eur. J.*
1079 *Immunol.* 44: 2638–2647.
- 1080 46. Stojanovic, A., N. Fiegler, M. Brunner-Weinzierl, and A. Cerwenka. 2014.
1081 CTLA-4 is expressed by activated mouse NK cells and inhibits NK Cell IFN- γ
1082 production in response to mature dendritic cells. *J. Immunol.* 192: 4184–4191.
- 1083 47. Koebel, C. M., W. Vermi, J. B. Swann, N. Zerafa, S. J. Rodig, L. J. Old,
1084 M. J. Smyth, and R. D. Schreiber. 2007. Adaptive immunity maintains occult
1085 cancer in an equilibrium state. *Nature* 450: 903–907.
- 1086 48. Fogel, L. A., W. M. Yokoyama, and A. R. French. 2013. Natural killer cells in
1087 human autoimmune disorders. *Arthritis Res. Ther.* 15: 216.
- 1088 49. Brahmer, J. R., S. S. Tykodi, L. Q. Chow, W. J. Hwu, S. L. Topalian, P. Hwu,
1089 C. G. Drake, L. H. Camacho, J. Kauh, K. Odunsi, et al. 2012. Safety and activity
1090 of anti-PD-L1 antibody in patients with advanced cancer. *N. Engl. J. Med.* 366:
1091 2455–2465.
- 1092 50. Dong, H., S. E. Strome, D. R. Salomao, H. Tamura, F. Hirano, D. B. Flies,
1093 P. C. Roche, J. Lu, G. Zhu, K. Tamada, et al. 2002. Tumor-associated B7-H1
1094 promotes T-cell apoptosis: a potential mechanism of immune evasion. *Nat. Med.*
1095 8: 793–800.
- 1096 51. Terme, M., E. Ullrich, L. Aymeric, K. Meinhardt, J. D. Coudert, M. Desbois,
1097 F. Ghiringhelli, S. Viaud, B. Ryffel, H. Yagita, et al. 2012. Cancer-induced
1098 immunosuppression: IL-18-elicited immunoablative NK cells. *Cancer Res.* 72:
1099 2757–2767.
- 1100 1101
1102
1103
1104
1105
1106
1107
1108
1109
1110
1111
1112
1113

AUTHOR QUERIES

AUTHOR PLEASE ANSWER ALL QUERIES

1

- 1—Please verify that the title, footnotes, author names, and affiliations are correct as set.
- 2—Please confirm the postal codes are correct as added to the affiliations.
- 3—Please confirm the Section of Hematology/Oncology is part of both the Department of Medicine and the Department of Pathology. The University website shows it as only part of the Department of Medicine. Please amend as needed.
- 4—Please note, the text “X.L.R.I., R.G.S., N.I.T., A.Z, R.E.A., F.S., and S.Y.N. are fellows of CONICET. J.M.S. is a fellow of the Instituto Nacional del Cancer. C.I.D., M.B.F., and N.W.Z. are members of the Researcher Career of CONICET” was moved to the grant footnote from *Acknowledgments* per journal style. Please also confirm phrasing “Researcher Career of CONICET.”
- 5—A response to this query is REQUIRED: ORCID (Open Researcher and Contributor ID) is a unique number used by researchers to unambiguously assign published work to the correct person. More information about it can be found here: www.orcid.org. Each author has the option to add his/her ORCID number to his/her profile in *The JI* online manuscript submission system. This ORCID number will be automatically added to a footnote in the accepted manuscript for any author who has added it to his/her profile. If this manuscript includes an ORCID footnote, the author(s) must confirm his/her ORCID number is correct. ORCID numbers should not be deleted without that author’s approval.
- 6—Please indicate the correct surname (family name) of each author for indexing purposes.
- 7—Please verify that the mailing address and e-mail address for correspondence are correct as set.
- 8—If your proof includes supplementary material, please confirm that all supplementary material is cited in the text.
- 9—If your proof includes links to Web sites, please verify that the links are valid and will direct readers to the correct Web page.
- 10—Any alternations between capitalization and/or italics in genetic nomenclature have been retained per the original manuscript. Please confirm that all genetic nomenclature has been formatted properly throughout.
- 11—In sentence beginning “For IFN- γ , CD107a, and tetramer staining, and for the identification/phenotypication. . .” please confirm spelling of “phenotypication”.
- 12—Per Journal style, please change “FoxP3” to be either FOXP3 (for human form) or Foxp3 (for murine form) at both appearances in the text.
- 13—A response to this query is REQUIRED: Please confirm that all potential conflicts of interest have been disclosed.

AUTHOR QUERIES

AUTHOR PLEASE ANSWER ALL QUERIES

2

- 14—Please advise, does the support mentioned in the edited *Acknowledgments* represent financial support? If so, it should be moved to the grant footnote, per Journal style.
 - 15—If your proof includes figures, please check the figures in your proof carefully. If any changes are needed, please provide a revised figure file.
 - 16—Please provide the value/significance of the quadruple (****) asterisks that appear in panel 5C.
-
-